STUDIA UNIVERSITATIS BABEŞ-BOLYAI BIOLOGIA, LXII, 1, 2017 (p. 29-42)
doi:10.24193/subbbiol.2017.1.02

SPION size dependent effects on normal and cancer cells

Sergiu Gabriel Macavei[1,2], Maria Suciu[2,3,✉], Izabell Crăciunescu[2,3], Lucian Barbu-Tudoran[2,3], Septimiu Cassian Tripon[2, 3], Cristian Leoştean[2] and Radu Bălan[1]

SUMMARY. Iron oxide nanoparticles have become widely used today in medical applications. In this study, we report a hyperthermia treatment with 10 and 100 nm naked and polyethylene glycol(PEG)-coated Super Paramagnetic Iron Oxide Nanoparticles (SPIONs) to normal and tumor cells in culture. Cells' responses to nanoparticles were analyzed by cell viability assays (MTT and LDH) and transmission electron microscopy. Results indicate that even if 10 nm SPIONs have good magnetization saturation, the hyperthermia treatment is not effective due to the fact that cells do not endocytose them. 100 nm SPIONs are better engulfed by cells, and their hyperthermia effect is slightly increased.

Keywords: hyperthermia, melanoma cells, SPION

Introduction

Nanoparticles are present in our every-day life, whether we like or not, whether we know it or not. We breathe micro and nanoparticles evacuated from cars exhaust pipes, we put them on our skin deliberately as sunscreens or cosmetics, or in our foods, we even have nanoparticles on our walls (Karjalainen *et al*., 2014; Smijs and Pavel, 2011; Das *et al*., 2011; Kaiser *et al*., 2013). We also use them in medicine for magnetic resonance imaging, as cytostatic enhancer or drug delivery system (Blasiak *et al*., 2013; Duan *et al*., 2016).

[1] *Department of Mechatronics and Machine Dynamics, Faculty of Mechanical Engineering, Technical University, 103-105 Muncii Bvd., 400641, Cluj-Napoca, Romania*
[2] *National Institute of Research and Development for Isotopic and Molecular Technologies, 67-103 Donath Str., 400293, Cluj-Napoca, Romania*
[3] *Faculty of Biology and Geology, Babes-Bolyai University, 5-7 Clinicilor Str., 400006, Cluj-Napoca, Romania*
✉ ***Corresponding author**: **Maria Suciu**, 5-7 Clinicilor Str., 400006, Cluj-Napoca*
E-mail: maria.suciu5@gmail.com

Super Paramagnetic Iron Oxide Nanoparticles (SPIONs) are currently used in medicine for magnetic resonance imaging and other types of imaging or as treatment for iron deficiency (Revia and Zhang, 2016). SPIONs are magnetite or maghemite nanoparticles that can be produced at desired dimensions and shapes, and can be covered with biocompatible materials and drugs or markers for various applications. SPIONs have the great advantage that they are biodegradable in the human body and a plus is that they have special magnetic properties. One of the many potential uses in medicine for SPIONs is for hyperthermia treatment. For this, SPIONs are placed in an alternating magnetic field which will determine SPIONs to produce heat that can be used for medical purposes (Bañobre-López *et al*., 2013; Giustini *et al*., 2010).

In this study, we explored the effect of size and PEG coverage on hyperthermia treatment *in vitro* on normal and cancer cells. Our results give proof to the fact that besides the magnetic properties of a nanoparticle, one should also consider the nanoparticle's dimension and surface coverage for the end effect of hyperthermia treatment on cells. These aspects are important for designing the most effective nanoparticles for hyperthermia treatments against cancer.

Materials and methods

Nanoparticles synthesis. For the 10 nm SPIONs synthesis we used the co-precipitation method of ferric and ferrous salts under the presence of argon gas (Turcu *et al.*, 2015). Our recipe was: 0.1 M $FeCl_3$ and 0.05 M $FeCl_2$ were dissolved into 200 mL of distilled water and stirred for 60 minutes. At 700 °C and under vigorous mixing we added 200 ml of 25 % NH_3 also under argon gas, and then left to precipitate for 2 h at pH of 12. After cooling to room temperature, the precipitates were magnetically separated, washed extensively with distilled water until neutral pH was reached. At the end, Fe_3O_4 magnetic nanoparticles were washed in acetone and dried at 60-70 °C. These resulted in 10 nm naked SPIONs.

SPIONs were then covered with PEG 2000 which produced the 10 nm SPION-PEG, considered to be biocompatible (Kostiv *et al*., 2017; Silva *et al*., 2016). For PEG coated SPIONs the recipe was as follows: 10 wt. % PEG and 1 wt. % of magnetic nanoparticles were mixed at room temperature, under vigorous magnetic stirring overnight in distilled water. Then SPIONs were magnetically separated and washed with distilled water and re-dispersed in water.

For the synthesis of 100 nm clusters of SPIONs, we used the oil in water mini-emulsion method (Crăciunescu *et al.*, 2017). Our recipe was as such: 0.5 wt% toluene based ferrofluid (Fe_3O_4) was added to an aqueous solution containing surfactant (sodium lauryl sulphate). This led to the formation of micelles dispersed in toluene.

This two-phase mixture was then homogenized using an ultrasonic finger for 2 minutes and the organic phase was evaporated under magnetic stirring (500 rpm), at 100^0 C in an oil bath. 100 nm SPIONs clusters were then washed with a methanol-water mixture to remove excess of reactants and re-dispersed in distilled water. These clusters represent the 100 nm naked SPIONs. From these we obtained the 100 nm PEG-coated SPIONs as described above.

TEM analysis of SPIONs. 10 and 100 nm SPIONs dispersed in water were placed on carbon coated 300 mesh copper grids. Multiple images were taken on a Hitachi STEM HD-2700 transmission electron microscope (TEM) at 200kV acceleration voltage.

VSM analysis of SPIONs. Room-temperature magnetic behavior of 10 and 100 nm SPIONs was recorded using a vibrating sample magnetometer (VSM) produced by "Cryogenic Ltd."

Cell culture procedures. For the hyperthermia study, we used normal human keratinocyte cells (HaCaT cell line), which was a gift from dr. Alina Sesarman, ICEI-BNS Cluj-Napoca, and human melanoma cells (A375 cell line) from ATCC. Keratinocytes were first cultured on plastic 25 cm^2 dishes in DMEM supplemented with 10% fetal calf serum, 1% penicillin-streptomycin and 1% L-glutamine. Melanoma cells were cultured according to the producer recommendations in 4.5 g/l glucose DMEM supplemented with 10% fetal calf serum, 1% penicillin-streptomycin and 1% L-glutamine. Cells were grown in a humidified incubator at 37 ºC and in a 5% CO_2 atmosphere. All cells were used when spread to 80% confluency, at which point they were trypsinized from the culture plate and seeded onto 96 wells plates for MTT and LDH analyses and on glass slides for TEM analysis.

A volume of 10 µl naked or PEG-coated SPIONs was added to cell media, at concentrations between 0.1 and 500 µg/ml. Their effects were tested at 24 hours of contact with the cells.

Hyperthermia treatment. For the hyperthermia induction, we used a Resistor-Inductor-Capacitor (RLC) circuit powered by a sinusoidal signal of an Arbitrary Waveform Generator type WW2571A and a custom-made power wide band amplifier having a frequency range of 100kHz-100MHz and a power range of RF 1-200W. Cells plated in 96 wells plate were incubated with the 10 and 100 nm SPIONs for 24 hours to ensure endocytosis. Plates were then placed in the alternating magnetic field for 20 minutes at 100 Oe and 0.75 MHz (for the 100 nm SPIONs) or 3 MHz (for the 10 nm SPIONs), and then returned to the incubator for another 24 hours. Before treatment, cell medium was replaced with fresh one to remove non-endocytosed

nanoparticles. The magnetic field for each type of nanoparticle was calculated according to their magnetization saturation (obtained by VSM) to the maximum power indicated by the Atkinson-Brezovich limit for human applications (Atkinson *et al*., 1984).

MTT method. Cells were seeded in 96 wells plate, at 12 x 10^3 cells/well density, and left to reach exponential phase for 24 hours. 10 or 100 nm SPION's were added to the culture media, and 24 hours later the mitochondrial activity was assessed by 3-(4,5-Dimethylthiazol-2-yl)-2,5-Diphenyltetrazolium Bromide (MTT) method. The MTT compound was added to each well to the final concentration of 0.5 mg/ml and left with the cells for 1.5 hours in the incubator. Afterwards, the media were removed and formazan crystals were lysed with acidified iso-propanol. The formazan absorbance was read at 550 nm (with background read at 630 nm) using BioTek Synergy HT plate reader and Gen5 Plate Reader Program (Riss *et al.*, 2016). Each concentration was tested six times and each plate contained untreated cells as positive control and negative controls (cells treated with Tween 20 2%). Data refers to mean ± standard error from at least three independent experiments. Comparison between control group and treated groups was performed with student's t-test and values of $p<0.05$ were considered significant; all calculations were performed in Microsoft Excel.

LDH method. For this method, we used 50 µl of culture medium from the MTT plates, which were transferred to a new 96 wells plate. To this we added 50 µl 50 mM lithium lactate solution, 50 µl 200 mM tris solution at pH 8, and 50 µl NAD solution. LDH reaction was read at 490 nm (with background at 690 nm) using BioTek Synergy HT plate reader and Gen5 Plate Reader Program (Chan *et al*., 2013). Data refers to mean ± standard error from at least three independent experiments. Comparison between control group and treated groups was performed with student's t-test and values of $p<0.05$ were considered significant; all calculations were performed in Microsoft Excel.

TEM analysis of cells and nanoparticles uptake. Cells were plated on 6 mm glass coverslips in a 12 wells plate. 100 µg/ml of 10 and 100 nm naked and PEG-coated SPIONs were added to cells and part of these glass coverslips were subjected to hyperthermia. 24 hours after the applied treatment, cells were fixed with 2.7% glutaraldehyde and post-fixed with 1% osmium tetroxide, dehydrated in ethanol, embedded in Epon resin and polymerized at 60 ºC. Samples were trimmed and ultrathin 50 nm sections were obtained using a Diatome diamond knife on Leica UC6 ultramicrotome. Sections were recovered on a carbon coated 200 mesh copper grids, and were left unstained and analyzed in a Jeol JEM 1010 TEM with MegaView II CCD Camera.

Results and discussion

In this study, we tested 10 and 100 nm SPIONs covered or un-covered with PEG in skin cell cultures. We used normal keratinocytes cells (HaCaT) and malignant melanoma (A375), since skin cells are daily subjected to all types of micro and nanoparticles from the surrounding environment. This fact is important because it gives us a better understanding of how the resistant cells might respond to the nanoparticle and hyperthermia treatments.

The TEM analysis of 10 and 100 nm SPIONs revealed the way nanoparticles look like at their nano sizes. In Fig. 1A, 10 nm SPIONs are imaged closely together due to physical forces that draw nanoparticles close when dried on the grid. Nanoparticles have around 8 to 12 nm and are well dispersed in water. No clumps were seen during analysis. The 100 nm SPIONs (Fig. 1B) are clusters of well defined spherical forms, having 70 to 150 nm diameters. In their structure, 10 nm magnetic nanoparticles can be identified. The 100 nm SPION clusters remained stable in their spherical form throughout the entire experimental procedures.

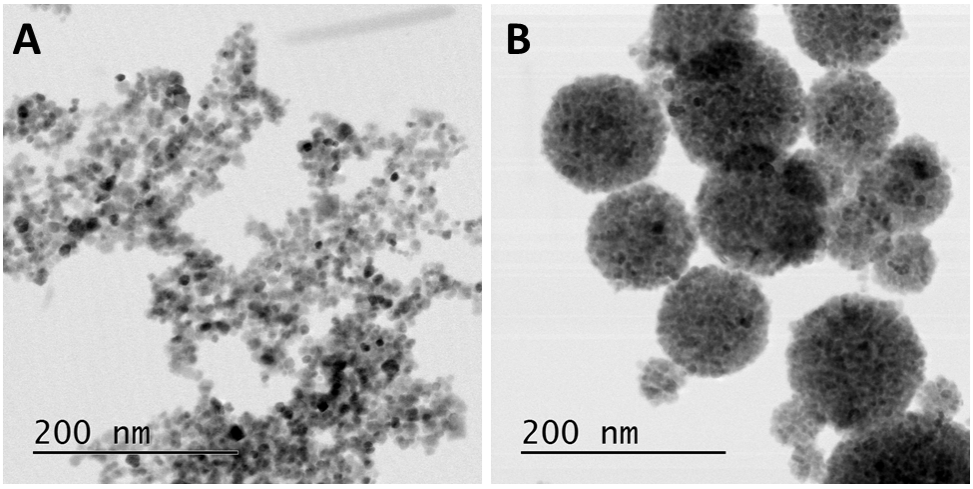

Figure 1. TEM micrographs of SPIONs. A - 10 nm SPIONs, B - 100 nm SPIONs.

The magnetization curves at room temperature of the SPION samples is shown in Fig. 2. As expected, the magnetization shows only a very small hysteresis loop, which is consistent with superparamagnetic behavior. The saturation magnetization (Ms) and coercitive field (Hc) values are 74.3 emu/g, 26 Oe for 10 nm SPIONs and 61.8 emu/g, 27 Oe for 100 nm SPIONs. The exchange field remains at low levels (<1 Oe). The lower value of Ms for the cluster structured 100 nm SPIONs is attributed to interparticle dipole-dipole interactions due to close packing.

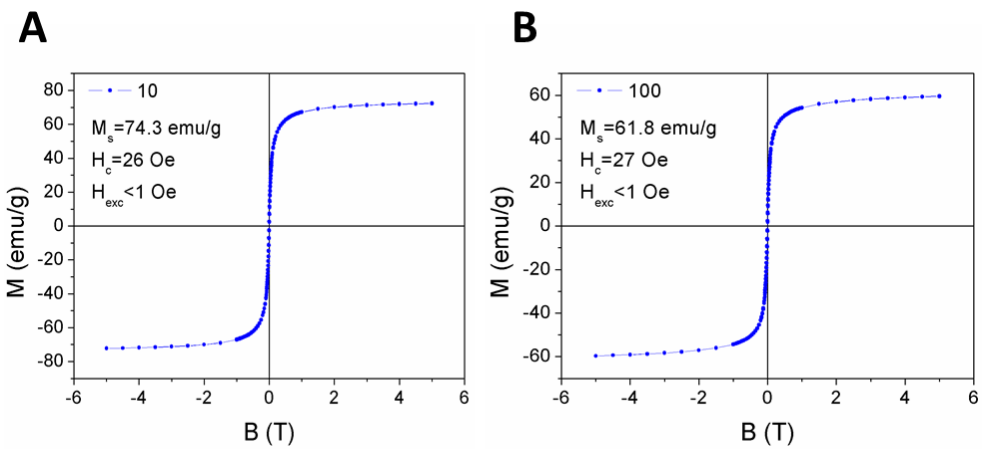

Figure 2. The magnetization curves versus applied magnetic field at room temperature of SPIONs. A - 10 nm SPIONs, B - 100 nm SPIONs.

The MTT analyses revealed that normal keratinocytes were not affected by the 10 nm naked SPIONs, as their mitochondrial activity was above 80% at all tested concentrations (0.1-500 µg/mL) and they were not affected even by the hyperthermia treatment (Fig. 3A, columns). On the contrary, the 10 nm PEG SPIONs, which are supposed to be biocompatible, reduced the mitochondrial activity of keratinocytes down to 50% (at the 10 µg/mL concentration). This reduction in the mitochondrial activity was not concentration dependent and gave different results in different separate MTT analyses. This, we believe, is due to the fact that when placed in contact with the cell culture medium, the nanoparticles clump together, are not well dispersed and therefore, are not uniformly endocytosed, giving different results. But what remains constant, though, is the fact that the 10 nm PEG SPIONs do reduce the cells' viability. When placed in a magnetic field, the mitochondrial activity remained reduced, although slightly higher than the cells not treated by hyperthermia (Fig. 3B, columns). This increase in the mitochondrial activity of the hyperthermia treated cells could be the result of 24 hours' time of recuperation from the contact with the SPIONs. Because, if the 10 nm naked SPIONs did not produce enough heating damage when subjected to magnetization, it is our belief that the PEG coating could not have raised the heating.

When placed in contact with the 100 nm naked SPIONs (Fig. 3C, columns), normal keratinocytes had a concentration dependent decrease in mitochondrial activity, remaining in the non-toxic percentage (100-80%) at 0.1 and up to 100 µg/mL, and dropping to 70% mitochondrial activity at the 500 µg/mL concentration. When placed

in the magnetic field, all concentration points dropped to 50-60% mitochondrial activity. The 100 nm PEG SPIONs (Fig. 3D, columns) gave a slightly reduced mitochondrial activity (80%) at the 500 µg/mL concentration, and non-toxic values for the other tested concentrations (0.1-100 µg/mL), even though somewhat variable (with large standard deviations). The hyperthermia treatment resulted in reduced mitochondrial activity to all tested concentrations, compared to same groups not treated by hyperthermia, with best results at 50 and 100 µg/mL concentrations (40-50% mitochondrial activity).

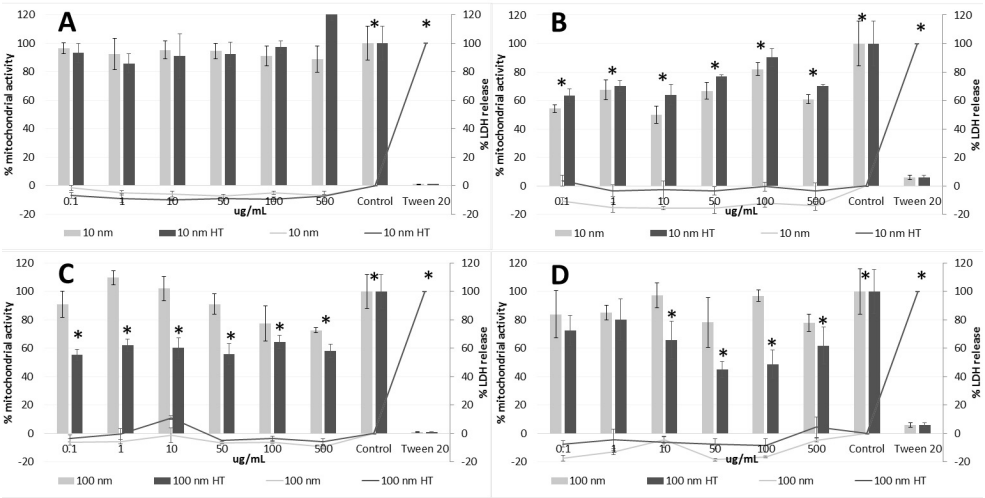

Figure 3. MTT and LDH analyses of normal keratinocytes treated with 10 and 100 nm SPIONs with and without hyperthermia. (A) 10 nm naked SPIONs; (B) 10 nm PEG SPIONs; (C) 100 nm naked SPIONs; (D) 100 nm PEG SPIONs. Columns represent mitochondrial activity values, and lines - LDH release percent values. Asterisks indicate statistical relevance between control and tested groups, $p<0.05$.

The human melanoma cells responded with a drop in their mitochondrial activity when put in contact with 10 nm naked SPIONs for 24 hours (Fig. 4A, columns). Values were between 60 and 70% mitochondrial activity in a concentration dependent manner. After the hyperthermia treatment, melanoma cells had a reduced mitochondrial activity (60-80%) starting from 10 to 500 µg/mL concentrations. The 10 nm PEG SPIONs gave a slightly reduced mitochondrial activity in the presence and absence of the magnetic field, in a concentration dependent manner, dropping below 80% from 10 µg/mL and reaching 60% at 500 µg/mL (Fig. 4B, columns).

Melanoma cells treated with 100 nm naked SPIONs had a reduced mitochondrial activity, down to 60-80%, independent of the administered concentrations. When cells were put in the alternating magnetic field, some were at the same mitochondrial level as without hyperthermia (0.1; 50 and 100 μg/mL), but some had higher mitochondrial activities (1; 10 and 500 μg/mL), with no evident pattern (Fig. 4C, columns). The 100 nm PEG-coated SPION gave a dose response mitochondrial activity, starting from non-toxic values (100-90%) concentrations (0.1-10 μg/mL) and ending at (80-70%) at 50-500 μg/mL. The cells treated by hyperthermia had a reduced mitochondrial activity (60-80%) at all concentrations (Fig. 4D, columns).

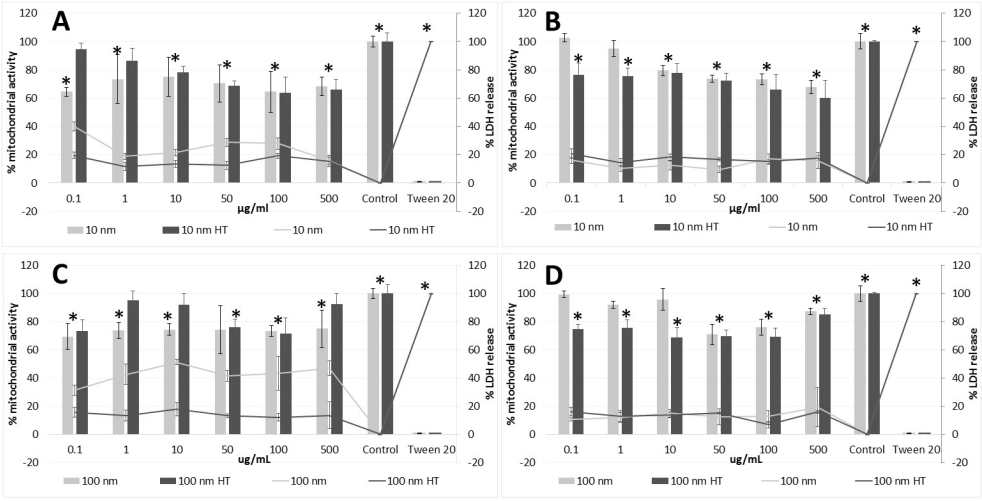

Figure 4. MTT and LDH analyses of melanoma cells treated with 10 and 100 nm SPIONs, with and without hyperthermia. (A) 10 nm naked SPIONs; (B) 10 nm PEG SPIONs; (C) 100 nm naked SPIONs; (D) 100 nm PEG SPIONs. Columns represent mitochondrial activity values, and lines - LDH release percent values. Asterisks indicate statistical relevance between control and treated groups, $p<0.05$.

LDH analyses showed no release for keratinocytes at any of the tested concentrations or conditions (with or without alternating magnetic field) under the action of 10 and 100 nm SPIONs, coated or uncoated with PEG. All values were around the untreated control values of release. Therefore, we can assume that these nanoparticles do not affect keratinocytes plasma membranes (Fig. 3, lines).

For the melanoma cells, LDH release had elevated values compared to keratinocytes. 10 nm naked nanoparticles produced a 20 to 40% LDH release at 24 hours of contact with cells, with the highest spike at 0.1 μg/mL and the lowest

value at 500 μg/mL concentration. After the hyperthermia treatment, the LDH release was lower (20%) and maintained constant throughout the concentrations (Fig. 4A, lines). In the case of PEG-coated 10 nm SPION, the LDH was 20% higher than the untreated cells' release, and remained constant at all concentrations, even under the effect of the magnetic field (Fig. 4B, lines).

The 100 nm naked SPIONs triggered the highest LDH release, ranging from 30 to 50% release (30% at 0.1 μg/mL and 50% at 10 and 500 μg/mL). This effect was not seen when put in the magnetic field, although it remained elevated to 20% at all concentrations (Fig. 4C, lines). The 100 nm PEG-coated SPIONs, again, produced an elevated LDH, but only just to 10-20%, throughout the entire concentrations and independent of the hyperthermia treatment (Fig. 4D, lines).

TEM analysis of cells treated with nanoparticles revealed the ultrastructural effects of SPIONs on normal and tumor cells. Both 10 nm and 100 nm SPIONs could be found in normal keratinocytes after 24 hours of exposure, some free in the cytoplasm, some contained in endosomes, but none of them reached the nuclei. Large groups of SPIONs could still be identified outside the cells, but attached to the cells' membranes. Endocytosed SPIONs were grouped in small clumps in which individual particles could be identified, meaning that the nanoparticles were not yet transformed to hemosiderin. Some evident derangement could be seen in keratinocytes exposed to 10 nm SPIONs for 24 hours (Fig. 5A): the cytoplasm was homogenous with constant, normal granulations, but in some places, there could be seen lysis areas of the cytoplasm, not surrounded by a membrane; mitochondria were scarce and swollen. Keratinocytes exposed to 100 nm SPIONs (Fig. 5B) had electron-dense cytoplasm packed with vesicles, and nuclei with homogenous chromatin. The strongly electron-dense cytoplasm and homogenous nuclei suggest protein synthesis problems, and the high number of cytoplasmic vesicles suggests an overdrive of cell functions (Panariti *et al*., 2012).

After the hyperthermia treatment, the cells were left to recover for 24 hours and the effects were ultrastructurally assessed. In the case of 10 nm SPIONs, most of the nanoparticles were located around the cells, only a few inside the cell and no evident differences could be seen between the hyperthermia treated and not-treated cells (Fig. 5C). It is possible that because of the reduced endocytosis, the heat produced by the 10 nm SPIONs placed in alternating magnetic field had dissipated into the cell culture media and did not affect the cell equilibrium. In the case of 100 nm SPIONs hyperthermia treated keratinocytes some differences could be discerned ultrastructurally (Fig. 5D): the number of intracellular SPIONs increased, the cell cytoplasm became much more electron-transparent than in the untreated cells, with large areas of undelimited lysis, and the nuclei contained a lot of euchromatin with many small patches of not so dense heterochromatin. SPIONs could be identified in the cytoplasm and in vesicles and also at cell borders, closely attached to cell membranes. Although the nanoparticle endocytosis process seems

to be more intense, in no cell sections could we find SPIONs internalized by caveolin or clathrin coated membrane pits, which we would expect for the nanoparticles sizes of 10 and 100 nm (Panariti *et al*., 2012).

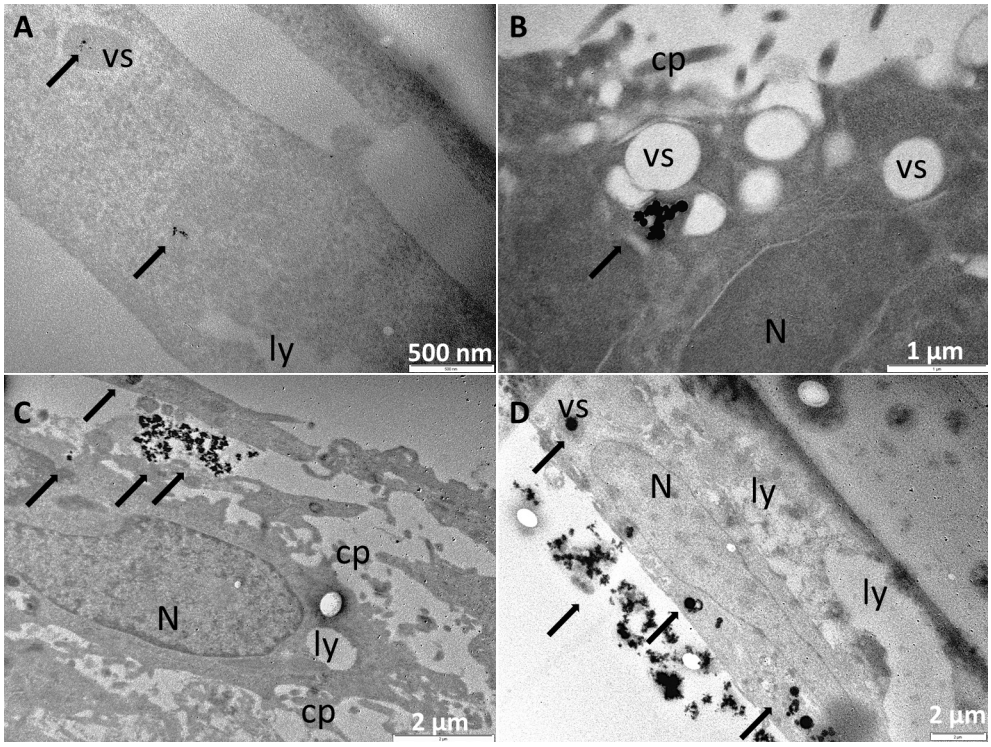

Figure 5. TEM micrographs of normal keratinocytes treated with SPIONs. (A) keratinocytes treated with 10 nm naked SPIONs for 24 hours; (B) keratinocytes treated with 100 nm naked SPIONs for 24 hours; (C) keratinocytes treated by hyperthermia with 10 nm naked SPIONs; (D) keratinocytes treated by hyperthermia with 100 nm naked SPIONs. vs- vesicle, ly - lysis, cp- cytoplasmic process, N- nucleus, arrow - SPIONs

Melanoma cells exposed to 10 and 100 nm SPIONs had a similar response in culture. Cells endocytosed a part of the SPIONs clumps but most of the nanoparticles were retained at the membrane surface (Fig. 6 A and B). The hyperthermia treated melanoma cells showed large areas of lysis in the cytoplasm, which could be located after the presence of the nanoparticles (Fig. 6 C and D).

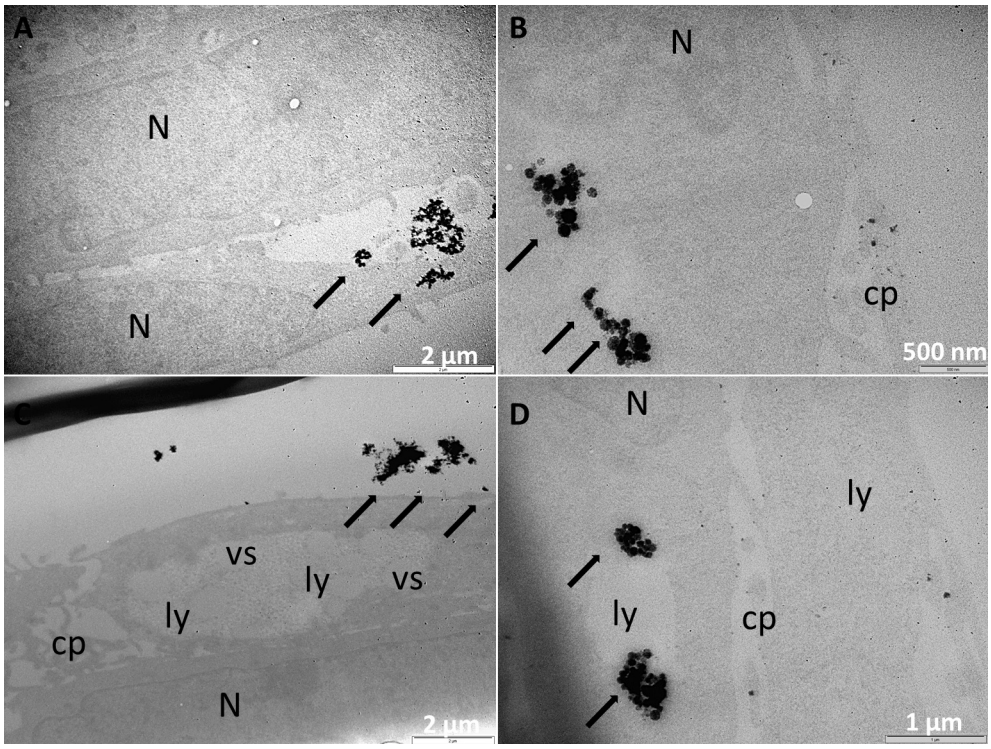

Figure 6. TEM micrographs of malignant melanoma treated with SPIONs. (A) melanoma treated with 10 nm naked SPIONs for 24 hours; (B) melanoma treated with 100 nm naked SPIONs for 24 hours; (C) melanoma treated by hyperthermia with 10 nm naked SPIONs; (D) melanoma treated by hyperthermia with 100 nm naked SPIONs.
vs- vesicle, ly - lysis, cp- cytoplasmic process, N- nucleus, arrow - SPIONs

SPIONs are studied more and more in the present, due to their proved biocompatibility and possibility of biotransformation into natural hemosiderin (Wu *et al*., 2010). Still, studies are controversial *in vitro* (Wahajuddin and Arora, 2012) and *in vivo* (Lee *et al*., 2008). Even if they are labeled as biocompatible, SPIONs still induce an array of cellular and/or medical problems, such as: toxicity by DNA or mitochondrial damage, capillary blockages, oxidative stress and other (Wahajuddin and Arora, 2012). In spite of this, we can find numerous types of iron oxide nanoparticles for sale, and used by physicians today for routine MRI and other applications (Stephen *et al*., 2011; Li *et al*., 2013; Estelrich *et al*., 2015).

Our results showed that 10 nm naked SPIONs are not toxic to normal keratinocytes even at high concentrations (500 µg/mL) but when covered with PEG the

cells' responses indicated mitochondrial stress. Instead, melanoma cells' mitochondrial activity was slightly affected by the 10 nm SPIONs independent of the used concentration and the presence/absence of PEG. PEG seemed to make a difference of action between cell types: keratinocytes had unaffected cell membranes when in contact with 10 nm SPIONs with or without PEG, but melanoma cells released more lactate dehydrogenase when SPIONs were un-covered with PEG. As the TEM analyses showed, these small SPIONs did not enter the cells in great amounts, at least not at the 24 hours' time point.

The 100 nm SPIONs, both covered and un-covered with PEG did not affect mitochondrial or membrane integrity of normal keratinocytes at either of the tested concentrations (0.1 - 500 μg/mL). But when placed in contact with melanoma cells, a relevant decrease in mitochondrial activity was revealed at all concentrations. The hyperthermia treatment affected keratinocytes greatly, and only slightly the melanoma cells (compared to cells not treated with hyperthermia). The improved magnetic hyperthermia response for the 100 nm SPIONs can be attributed to dipolar interaction typical to structured clusters (Coral *et al*., 2016). Another noticeable difference identified was the fact that after the hyperthermia treatment more 100 nm SPIONs were found in both cell types. This could be due to the physical stress induced by the hyperthermia over the cell membranes or due to the fact that, together with the hyperthermia treatment, the total amount of time of cell contact was 48 hours till the endpoint analyses.

Conclusions

In the case on superparamagnetic iron oxide nanoparticles, size matters. It matters for the endocytosis process and for the cells' response to hyperthermia treatment. What also matters is the nanoparticle structure (simple vs. cluster), and the presence of PEG on the surface of these nanoparticles, as some cells might be affected in the absence of PEG (such as melanoma cells membranes, in our case) and other might be affected by its presence (keratinocytes mitochondria, in our case).

Through our study, we showed that different cell types responded differently to hyperthermia treatment, not entirely dependent on the magnetization saturation of the nanoparticles but also on size, structure and surface coverage. These aspects finely tuned for a specific type of cell could make the difference to the final effect of the hyperthermia treatment.

Acknowledgements. This work was supported by the Romanian National Authority for Scientific Research and Innovations, CNCS-UEFISCDI, project number PN2-RU-TE-2014-4-0608 and by the 544644-TEMPUS-1-2013-1-UK-TEMPUS-JPCR Project. We thank A. Sesarman, PhD, for the HaCaT cells and Dumitrita Rugina, PhD, for the access to cell culture infrastructure.

REFERENCES

Atkinson, W. J., Brezovich, I. A., Chakraborty, D. P. (1984) Usable frequencies in hyperthermia with thermal seeds, *IEEE Trans. Biomed. Eng*. **31**:70–75

Bañobre-López, M., Teijeiro, A., Rivas, J. (2013) Magnetic nanoparticle-based hyperthermia for cancer treatment, *Reports of Practical Oncology & Radiotherapy,* **18**(6):397–400

Blasiak, B., van Veggel, F. C. J. M., Tomanek, B. (2013) Applications of Nanoparticles for MRI Cancer Diagnosis and Therapy, *Journal of Nanomaterials,* **2013***:* 12

Chan, F. K. -M., Moriwaki, K., De Rosa, M. J. (2013) Detection of Necrosis by Release of Lactate Dehydrogenase (LDH) Activity, *Methods in molecular biology,* **979**:65-70

Coral, D. F., Mendoza Zélis, P., Marciello, M., del Puerto Morales, M., Craievich, A., Sánchez, F. H., Fernández van Raap, M. B. (2016) Effect of Nanoclustering and Dipolar Interactions in Heat Generation for Magnetic Hyperthermia, *Langmuir*, **32**(5):1201–1213

Craciunescu, I., Petran, A., Liebscher, J., Vekas, L., Turcu, R. (2017) Synthesis and characterization of size-controlled magnetic clusters functionalized with polymer layer for wastewater depollution, *Materials Chemistry and Physics*, **185**:91–97

Das, M., Ansari, K. M., Tripathi, A., Dwivedi, P. D. (2011) Need for safety of nanoparticles used in food industry, *J. Biomed. Nanotechnol.,* **7**(1):13-4

Duan, X., He, C., Kron, S. J., Lin, W. (2016) Nanoparticle formulations of cisplatin for cancer therapy. *WIREs Nanomed Nanobiotechnol*, **8**: 776–791

Estelrich, J., Sánchez-Martín, M. J., Busquets, M. A. (2015) Nanoparticles in magnetic resonance imaging: from simple to dual contrast agents, *International Journal of Nanomedicine*, **10**:1727–1741

Giustini, A. J., Petryk, A. A., Cassim, S. M., Tate, J. A., Baker, I., Hoopes, P. J. (2010) Magnetic Nanoparticle Hyperthermia In Cancer Treatment, *Nano LIFE*, **1:**(01n02)

Kaiser, J. -P., Diener, L., Wick, P. (2013) Nanoparticles in paints: A new strategy to protect façades and surfaces?, *Journal of Physics: Conference Series,* **429**:012036

Karjalainen, P., Pirjola, L., Heikkilä, J., Lähde, T., Tzamkiozis, T., Ntziachristos, L., Keskinen, J., Rönkkö, T. (2014) Exhaust particles of modern gasoline vehicles: A laboratory and an on-road study, *Atmospheric Environment,* **97**:262–270

Kostiv, U., Patsula, V., Šlouf, M., Pongrac, I. M., Škokić, S., Dobrivojević Radmilović, M., Pavičić, I., Vinković Vrček, I., Gajović, S., Horák, D. (2017) Physico-chemical characteristics, biocompatibility, and MRI applicability of novel monodisperse PEG-modified magnetic Fe3O4&SiO2 core–shell nanoparticles, *RSC Adv.,* **7**:8786-8797

Lee, J. -H., Schneider, B., Jordan, E. K., Liu, W., Frank, J. A. (2008) Synthesis of Complexable Fluorescent Superparamagnetic Iron Oxide Nanoparticles (FL SPIONs) and Cell Labeling for Clinical Application, *Advanced Materials,* **20**(13):2512–2516

Li, L., Jiang, W., Luo, K., Song, H., Lan, F., Wu, Y., Gu, Z. (2013) Superparamagnetic Iron Oxide Nanoparticles as MRI contrast agents for Non-invasive Stem Cell Labeling and Tracking, *Theranostics*, **3**(8):595–615

Panariti, A., Miserocchi, G., Rivolta, I. (2012). The effect of nanoparticle uptake on cellular behavior: disrupting or enabling functions?, *Nanotechnology, Science and Applications*, **5**:87–100

Revia, R. A., Zhang, M. (2016) Magnetite nanoparticles for cancer diagnosis, treatment, and treatment monitoring: recent advances, *Materials Today,* **19**(3):157–168

Riss, T. L., Moravec, R. A., Niles, A. L., Duellman, S., Benink, H. B., Worzella, T. J., Minor, L. (2016) Cell Viability Assays, In: *Assay Guidance Manual*, Sittampalam, G. S., Coussens, N. P., Nelson, H., *et al*. (eds.), Eli Lilly & Company and the National Center for Advancing Translational Sciences Bethesda, pp. 1-30

Silva, A. H., Lima, E. Jr., Mansilla, M. V., Zysler, R. D., Troiani, H., Pisciotti, M. L., Locatelli, C., Benech, J. C., Oddone, N., Zoldan, V. C., Winter, E., Pasa, A. A., Creczynski-Pasa, T. B. (2016) Superparamagnetic iron-oxide nanoparticles mPEG350- and mPEG2000-coated: cell uptake and biocompatibility evaluation, *Nanomedicine*, **12**(4):909-19

Smijs, T. G., Pavel, S. (2011) Titanium dioxide and zinc oxide nanoparticles in sunscreens: focus on their safety and effectiveness, *Nanotechnology, Science and Applications,* **4**:95–112

Stephen, Z. R., Kievit, F. M., Zhang, M. (2011) Magnetite Nanoparticles for Medical MR Imaging. *Materials Today*, **14**(7-8): 330–338

Turcu, R., Socoliuc, V., Craciunescu, I., Petran, A., Paulus, A., Franzreb, M., Vasile, E., Vekas, L. (2015) Magnetic microgels, a promising candidate for enhanced magnetic adsorbent particles in bioseparation: synthesis, physicochemical characterization, and separation performance, *Soft Matter,* **11**:1008-1018

Wahajuddin, S. A., Arora, S. (2012) Superparamagnetic iron oxide nanoparticles: magnetic nanoplatforms as drug carriers, *International Journal of Nanomedicine*, **7**:3445–3471

Wu, E. X., Kim, D, Tosti, C. L., Tang, H., Jensen, J. H., Cheung, J. S., Feng, L., Au, W. Y., Ha, S. Y., Sheth, S. S., Brown, T. R., Brittenham, G. M. (2010) Magnetic resonance assessment of iron overload by separate measurement of tissue ferritin and hemosiderin iron, *Annals of the New York Academy of Sciences*, **1202**:115-122